Solid State Communications 153 (2013) 13–16

Contents lists available at SciVerse ScienceDirect

Solid State Communications

journal homepage: www.elsevier.com/locate/ssc

The study of local atomic and electronic structure with magnetic properties of $Bi(Fe_{0.95}Co_{0.05})O_3$ ceramics

Yongtao Li [a,b,c], Hongguang Zhang [a,c], Hao Liu [a,c], Qi Li [a,c,*], Xing'ao Li [b], Weiwei Mao [b], Xingfu Wang [b], Qingyu Xu [a], Shiqiang Wei [c]

[a] Department of Physics, Southeast University, Nanjing 211189, PR China
[b] Experimental Teaching Center of Physics, Nanjing University of Posts and Telecommunications, Nanjing 210003, PR China
[c] National Synchrotron Radiation Laboratory, University of Science and Technology of China, Hefei 230029, PR China

ARTICLE INFO

Article history:
Received 1 April 2012
Received in revised form
16 July 2012
Accepted 6 October 2012
by M. Wang
Available online 13 October 2012

Keywords:
A. Multiferroic
D. Magnetism
C. Local structure
E. XAFS

ABSTRACT

The origin of the room-temperature ferromagnetism of $Bi(Fe_{1-x}Co_x)O_3$ ($x=0$, 0.05) has been investigated by X-ray Absorption Fine Structure (XAFS) and Soft X-ray Absorption Spectroscopy (SXAS). The results of XAFS data indicate that partial Fe cations occupy Bi-sites of lattices and the dopant Co cations occupy Fe-sites. The existence of divalent Fe^{2+} ions in this system is detected. The O1*s* core level SXAS spectra indicate the crystal field split energy for $x=0.05$ sample is larger than that for $x=0$ sample, which means a structural distortion. The origin of ferromagnetism in both samples is related to the existence of Fe^{2+} ions, crystal lattice distortion and occupation of Fe ions. To the enhancement of saturated magnetizations in the Co-doped sample, the existence of Fe^{2+} ions is not the dominant factor, while the crystal lattice distortion due to partial Fe ions occupying at Bi-sites plays an important role.

1. Introduction

The family of ABO_3 (for some instance, A=Bi; B=Fe, Mn) perovskite oxide compounds constitutes an important class of multifunctional materials which, within same simple cubic structure, exhibit a wide variety of behaviors (for example, ferroelectric, piezoelectric, nonpolar antiferrodistorted insulators, metals, and superconductors) and an additional magnetic order [1–2]. The material $BiFeO_3$ (BFO), as one of a few multiferroic materials, has attracted increasing interest due to its high ferroelectric Curie temperature ($T_C \sim 1100\,K$) and high antiferromagnetic Néel temperature ($T_N \sim 650\,K$), which appears to have good potential applications such as information storage, spintronics, and sensors [3–5]. Recently, metallic element cobalt was doped into $BiFeO_3$ to enhance ferromagnetism, but the origin of the enhancement of the saturated magnetization (M_S) is not clear [6]. Some reports have been published in recent years dealing with the observation of magnetic properties of BFO with various A site and B-site (Bi and Fe-sites of BFO, respectively, whose crystal structure is rhombohedrally distorted perovskite ABO_3) substitutions [7–8]. The possible origin of ferromagnetism in doped multiferroic BFO materials may be attributed to either the existence of divalent Fe^{2+} ions (induced by the oxygen vacancies [9] or doping ions [10]) or a small distortion in the Fe^{3+}–O–Fe^{3+} spin arrangement [11].

X-ray Absorption Fine Structure (XAFS) [12–13] has been developed for determining the inversion parameters of multiferroic materials [14–15]. XAFS, which is a modern powerful tool for local structure studies, provides a good method of obtaining local structural information of the materials, as well as interatomic distances, coordination number, and so on. The local structure information of atoms around a selected X-ray absorbing atom can be obtained by analyzing the XAFS spectra, which can provide fundamental details in order to understand the change of magnetic properties of these compounds. In this article, the local atomic structures and electronic structures of $Bi(Fe_{1-x}Co_x)O_3$ ($x=0$, 0.05) samples detected by XAFS and Soft X-ray Absorption Spectroscopy (SXAS) of Fe 2*p* and O 1*s* core levels are studied so that the origin of the change in magnetic properties [6] may be found out.

2. Experimental details

$Bi(Fe_{1-x}Co_x)O_3$ ($x=0$, 0.05) bulk ceramics were prepared by rapid sintering sol–gel method. The X-ray diffraction patterns and the magnetization of $Bi(Fe_{1-x}Co_x)O_3$ ($x=0$, 0.05) were measured

* Corresponding author at: Department of Physics, Southeast University, Nanjing 211189, PR China. Tel.: +86 25 52090600x8307; fax: +86 25 52090600x8203.
E-mail address: qli@seu.edu.cn (Q. Li).

0038-1098/$ - see front matter © 2012 Elsevier Ltd. All rights reserved.
http://dx.doi.org/10.1016/j.ssc.2012.10.005

by Xu et al. [6]. The X-ray diffraction patterns showed smaller lattice parameters of $BiFe_{0.95}Co_{0.05}O_3$ (a=0.3959 nm and α=89.48°) than those of $BiFeO_3$ (a=0.3976 nm and α=89.59°). The magnetization of $Bi(Fe_{1-x}Co_x)O_3$ (x=0, 0.05) was measured by a vibrating sample magnetometer integrated in a physical property measurement system (PPMS-9, Quantum Design). The magnetic properties of $Bi(Fe_{1-x}Co_x)O_3$ (x=0, 0.05) exhibited an increasing trend with increasing the content of cobalt ions. The mechanism of this enhancement of magnetism may be related to cationic distributions as analyzed below.

The X-ray absorption fine structure (XAFS) spectra of these multiferroic samples were measured at beamline U7C at National Synchrotron Radiation Laboratory (NSRL), University of Science and Technology of China (USTC). The data of X-ray absorption for each sample were collected in transmission mode with ionization chambers with Ar/N_2 filled gas at room-temperature. Harmonics were rejected by using a grazing incidence mirror. The X-ray beam was monochromatized using a Si(111) crystal in the energy range 6961–8112 eV (The Fe K-edge energy is 7112 eV). Data analysis was performed using USTCXAFS2.0 code [16–17]. The XAFS oscillation signals were extracted after background subtraction of raw data and were normalized by the edge height around 50–300 eV above the threshold. The Fourier transforms of Fe K-edge were performed over the k range of 35 $nm^{-1} < k < 125$ nm^{-1}. The measurement of SXAS of Fe2p and O1s core levels in total electron yield mode were performed at room-temperature at Beijing Synchrotron Radiation Facility (BSRF).

3. Results and discussions

The X-ray absorption fine structure spectra of Fe K-edge of the prepared two samples are shown in Fig. 1. From this figure, it can be seen that the spectra shape and peak position of two samples are almost same indicating the mainly identical local atomic structure. A little change in the spectra is observed that the absorption threshold energy of Fe K-edge is slightly different. And the threshold energy of the sample with x=0.05 (7124.58 eV) shifts to higher energy side compared to the sample with x=0 (7121.23 eV), which may demonstrate that the whole valence states of Fe ions in x=0.05 is higher than that in x=0. This point can be proved by the SXAS of Fe 2p core level. To study the local atomic structure, Fe k-edge k^3-weighted XAFS curves of $Bi(Fe_{1-x}Co_x)O_3$ (x=0, 0.05) are given in Fig. 2. It is found that the Fe K-edge XAFS spectra of the samples look similar to each other at the region of lower k, but they are different at higher k region. For instance, the peak at around 110 nm^{-1} splits into two peaks and the peak at around 114 nm^{-1} weakens with doping Co ions. It implies to some extent that the local structure of center atoms has changed owing to adding cobalt cations.

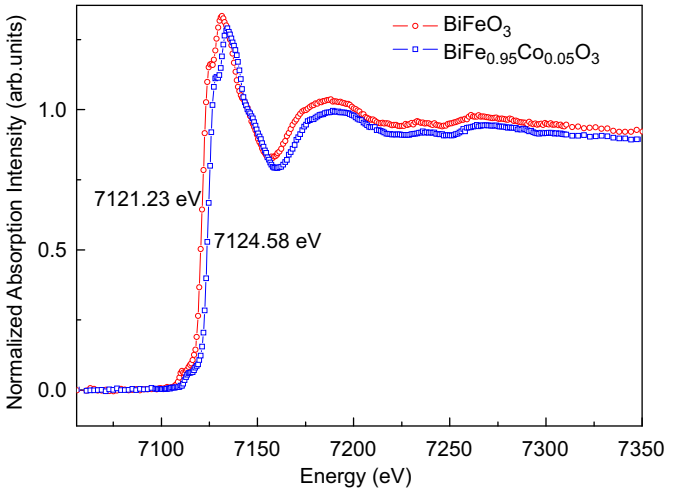

Fig. 1. (Color online) The normalized X-ray absorption fine structure spectra of $Bi(Fe_{1-x}Co_x)O_3$ (x=0, 0.05) at Fe K-edge.

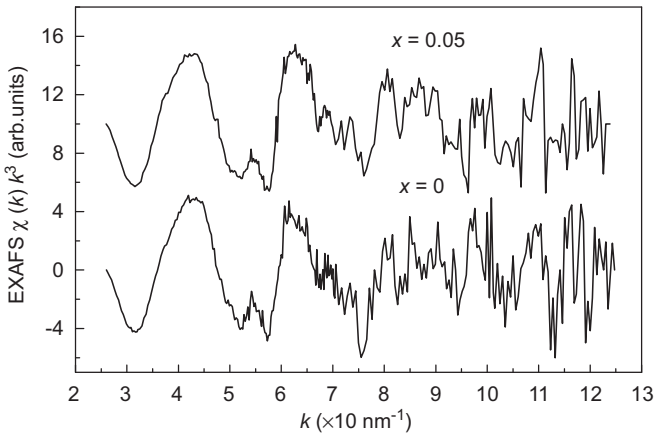

Fig. 2. Fe K-edge k^3-weighted XAFS of $Bi(Fe_{1-x}Co_x)O_3$ (x=0, 0.05).

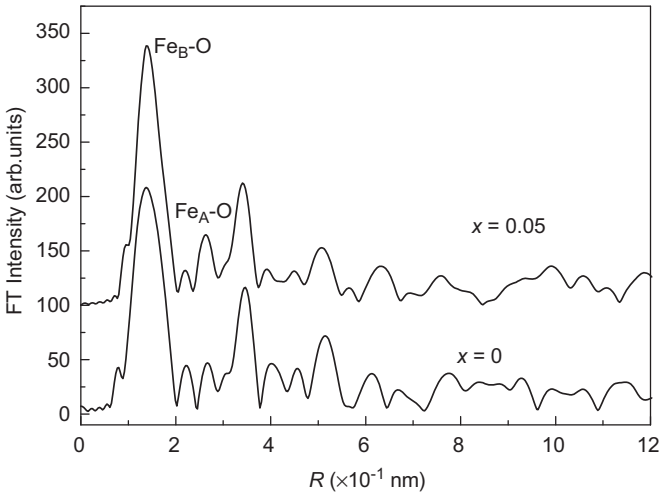

Fig. 3. Fourier transforms of Fe K-edge k^3-weighted XAFS for $Bi(Fe_{1-x}Co_x)O_3$ (x=0, 0.05). The Fe_B–O peaks and the Fe_A–O peaks arise from scattering from which are centered Fe ions at B sites and A sites, respectively.

Fourier transforms for Fe K-edge k^3-weighted XAFS of the samples are performed, as presented in Fig. 3. The asymmetric Fe–O peak that is centered near 0.15 nm arises from scattering from the nearest neighbor atomic shell of Fe, i.e., oxygen anions; the second intense peak around 0.35 nm is caused by scattering from the second nearest neighbors, i.e., the metal cations. These two major peaks in the figure are the signals from the first nearest neighbor and the second nearest neighbor of iron ions, which are assigned to Fe–O bonding and Fe–Fe/Co bonding, respectively.

With Co doping, as to the peak positions concerned, the distance between the central atoms and the second nearest atoms does not vary too much, it may be due to the almost same ion radius between Fe and Co ions (R^{3+}_{Fe}=0.064 nm, R^{3+}_{Co}=0.063 nm). However, the positions of the peaks around 0.35 nm slightly shift to lower R, resulting in diminishment of lattice constant, in consistent with the results of XRD [6]. This shift of the peak positions around 0.35 nm in Fig. 3 may be attributed to the decrease of both the amount of divalent Fe ions and that of oxygen vacancies in the samples. It should be noticed that the peaks at around 0.26 nm, which arise from Fe ions at Bi-sites, are observed.

The intensities of the peaks increase with doped cobalt composition, which reflects the incorporation of partial Fe ions into Bi-site of the lattice and the content of Fe ions at Bi-sites increases. This result may come from the preparation process (the samples are rapidly sintered). The coordination number N of Fe ion is obtained by fitting the first shell oscillation signal with FEFF 7.0 program. The value of N for $x=0$ and $x=0.05$ is 6.06 and 6.56, respectively, which means that the ratio of Fe ions occupied Bi-sites relative to the whole Fe ions is about 0.8% and 9.4% (due to the coordination number N of Fe ions at Fe-site and Bi-site is 6 and 12 in this perovskite structure).

To prove the existence of divalent Fe^{2+} ions, the Fe 2p core level SXAS spectra of two prepared samples are shown in Fig. 4. It can be seen that the two peaks at energy position near 710 and 723 eV are observed in each spectra, which comes from the spin–orbit split. As to these broad peaks, each has a main peak and a shoulder, and the broad peaks can be deconvoluted into two peaks. For example, it can be clearly seen that in the $2p_{3/2}$ peak two obvious peaks exist, as shown in Fig. 4 with labeled bars. As to the energy position, it indicates the mixed valence states (Fe^{2+} and Fe^{3+}) of Fe ions. Compared to the sample $x=0$, the peak position of these $2p_{3/2}$ peak in $x=0.05$ sample shows a shift to higher photon energy side with 0.8 eV, indicating the increase of whole mixed valence states. In other words, the amount of divalent Fe^{2+} ions decreases with increasing x, which is consistent with the results given by XAFS in Fig. 1.

The O1s SXAS spectra of two prepared samples are also investigated as shown in Fig. 5. The O1s SXAS spectra in BFO samples are attributed to the transitions from O1s to O2p [18]. The peaks labeled a, b and c in the figure are the fitted results with three electronic configuration states using Gaussian function. The peaks a, b, and c correspond to the t_{2g} and e_g states of Fe3d state and Bi 6sp state, respectively [19]. The crystal field split energy $\Delta E=E(e_g)-E(t_{2g})$ are 1.43 and 1.62 eV for $x=0$ and 0.05, respectively. This increase of crystal field split energy indicates the distortion of lattice structure, which is consistent with the results of XAFS.

As to the variation of M_S for the series of samples, it can be explained in the way as following. Divalent Fe ions exhibited in both the two samples may be caused by oxygen vacancies as obtained by XAFS and SXAS. A net magnetic moment is caused by the ferrimagnetic alignment of Fe^{2+} ions moments opposite to that of the Fe^{3+} ions [20], which can explain the existence of room-temperature ferromagnetism in both samples [9]. However,

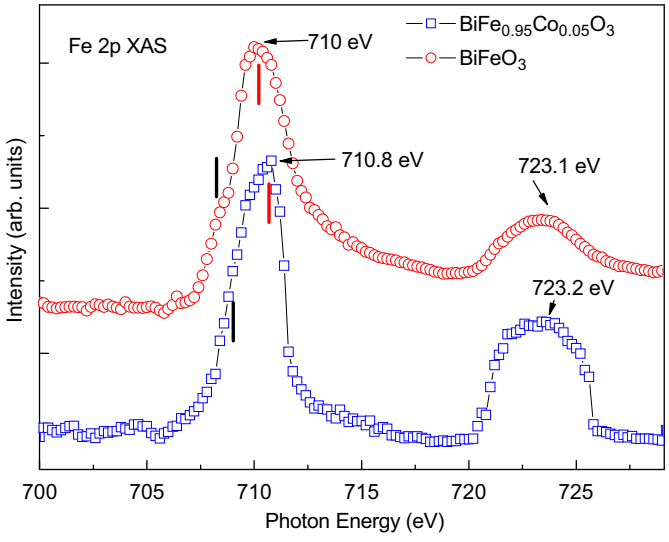

Fig. 4. (Color online) The soft x-ray absorption spectroscopy of Fe 2p core level in samples $Bi(Fe_{1-x}Co_x)O_3$ ($x=0$, 0.05).

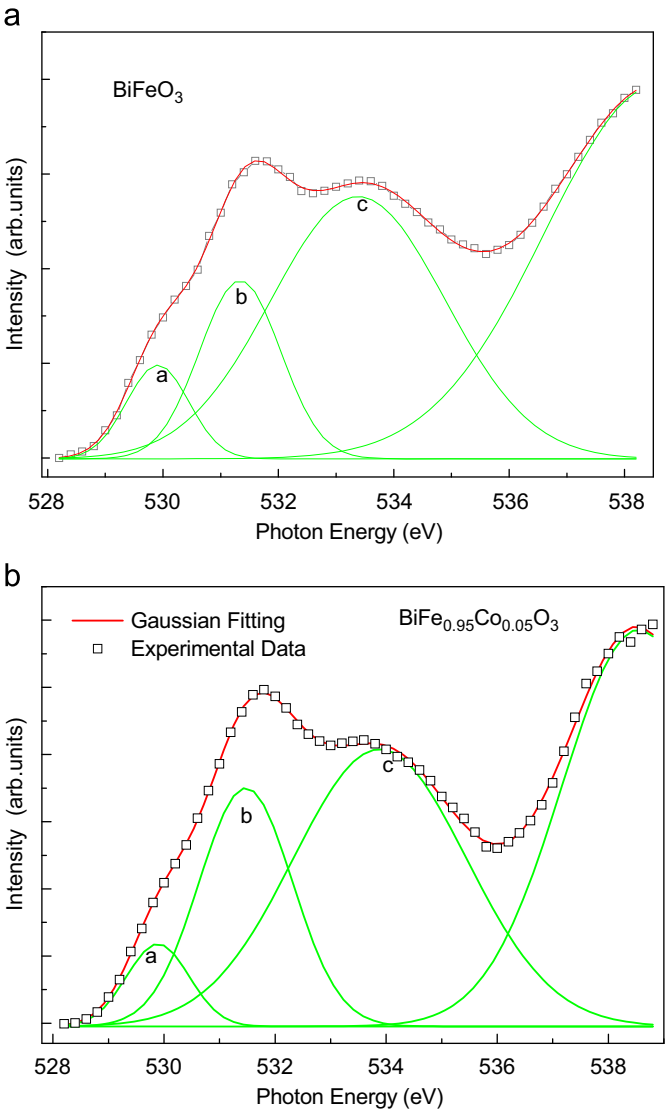

Fig. 5. (Color online) The soft X-ray absorption spectroscopy of O 1s core level of samples $Bi(Fe_{1-x}Co_x)O_3$ ($x=0$ (a), 0.05 (b)). The curves labeled a, b, c in each figure are the fitted curves with Gaussian function.

the concentration of divalent Fe ions is less in $x=0.05$ than that in $x=0$, because of the increase of whole valence states in the system as detected by the XAFS and SXAS. As to the enhancement of ferromagnetism in Co-doped sample, thus it can be concluded that the existence of divalent Fe^{2+} ions is not the dominant factor for the enhancement of room-temperature ferromagnetism. The origin of such enhancement in magnetization may be attributed to the substitution of Co ions for Fe ions in the system, which destroys the spatially inhomogeneous spin-modulated asymmetric structure and increases the spin canting angle leading to a net magnetization [21–22].

In our two prepared samples, that parts of Fe ions occupy Bi-sites has been detected by the radial structure function curves, as shown in Fig. 3. Therefore, parts of Fe–O–Fe bonds may present states of nearly vertical arrangements as illustrated in Fig. 6, which can explain the ferromagnetism in terms of superexchange interaction through Fe–O–Fe with 90°. An antiferromagnetism is usually induced by superexchange interaction when angle in Fe–O–Fe bonds is close to 180°. And the ferromagnetism can be yielded when angle in Fe–O–Fe bonds is close to 90° [11]. And as to the Co-doped sample, the content of Fe ions occupied cations at Bi-site is more than that of sample $x=0$. The magnetic ordering of

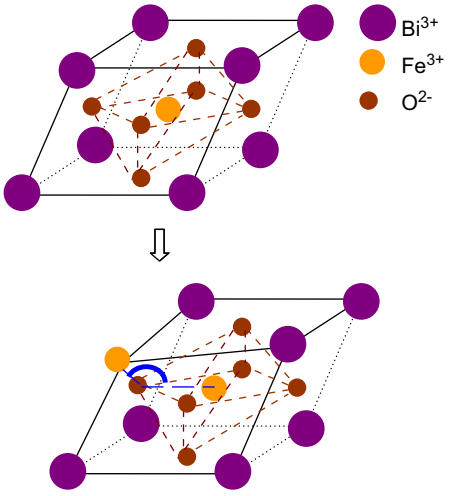

Fig. 6. (Color online) The scheme that parts of Fe–O–Fe bond may present states on Co-doped $BiFeO_3$.

this series of samples is essentially *G*-type antiferromagnetic with cycloidal spin magnetic ordering [23]. The magnetic moments of the Fe cations produce antiparallel alignment, before doping Co cations. When cobalt cations have been doped into $BiFeO_3$ sample, a few trivalent Fe cations at Fe-sites are replaced by Co cations, and a small part of Fe cations have occupied Bi-sites, which is confirmed by the analysis of XAFS data. Partial Fe cations occupied Bi-sites probably turn antiferromagnetism, which is intrinsic to BFO, into weak ferromagnetism with Co doping at the Fe-sites, because of a collapse of the space-modulated spin structure. The ferromagnetism can be significantly improved since the doping of Co ions changes the *G*-type antiferromagnetic order of the magnetic moments for the metallic cations at Fe-sites into ferromagnetic ones. The origin of magnetization enhancement thus can be accounted for on the basis of cation distribution. Except that, the O1*s* SXAS spectra give the information that the crystal field split energy of $x=0.05$ is larger than that of $x=0$, which indicates more distortion of lattice structure. From this point, the bond angle of parts of Fe ions taking place of cations at Bi-site is distorted, inducing spin canting and leading to the enhancement of saturated magnetization.

4. Conclusions

In summary, the magnetic properties of multiferroic material $Bi(Fe_{1-x}Co_x)O_3$ ($x=0$, 0.05) prepared with rapid sintering method have been investigated by XAFS and SXAS. It is noted that, with increasing Co substitution, an enhanced magnetization has been observed in BFO. The local structures of $Bi(Fe_{1-x}Co_x)O_3$ ($x=0$, 0.05) samples have been investigated with the XAFS technique. The results of XAFS data demonstrate that partial Fe cations occupy A sites of lattices and the dopant Co cations occupy B sites. The Fe 2*p* core level SXAS indicates the existence of divalent Fe^{2+} ions in the system which may be caused by oxygen vacancies. The O1*s* core level SXAS demonstrates that the crystal field split energy in $x=0.05$ sample is larger than that in $x=0$ sample, which means the distortion of lattice structure. From above, the origin of ferromagnetism in both samples is related to the existence of Fe^{2+} ions, crystal lattice distortion and occupation of Fe ions. As to the enhancement of saturated magnetizations in the Co-doped sample, the existence of Fe^{2+} ions is not the dominant factor, and both partial Fe ions occupying the A site and crystal lattice distortion play the most important role.

Acknowledgments

We are indebt to NSFC for its financial support to our research projects Nos. 10979016 and 51172110, and to NSRL and BSRF for their beamtime, and to NSRL for its support to our research project Graduate Student Innovation Fund under Grant no. 20090621S. Furthermore, this work is also supported by Nanjing University of Posts and Telecommunications in research project of NY211144.

References

[1] A.B. Posadas, M. Lippmaa, F.J. Walker, M. Dawber, C.H. Ahn, J. Triscone, Top. Appl. Phys. 105 (2007) 219.
[2] J. Wang, et al., Science 299 (2003) 1719.
[3] C. Michel, et al., Solid State Commun. 7 (1969) 701.
[4] N.A. Hill, J. Phys. Chem. B 104 (2000) 6694.
[5] M. Fiebig, et al., Nature 419 (2002) 819.
[6] Q. Xu, H. Zai, D. Wu, T. Qiu, M.X. Xu, Appl. Phys. Lett. 95 (2009) 112510.
[7] V.R. Palkar, D.C. Kunkaliya, S.K. Malik, S. Bhattacharya, Phys. Rev. B 69 (2004) 212102.
[8] D.H. Wang, W.C. Goh, M. Ning, C.K. Ong, Appl. Phys. Lett. 88 (2006) 212907.
[9] Y. Li, T. Sritharan, S. Zhang, X. He, Y. Liu, T. Chen, Appl. Phys. Lett. 92 (2008) 132908.
[10] F. Gao, C. Cai, Y. Wang, S. Dong, X.Y. Qiu, G.L. Yuan, Z.G. Liu, J.M. Liu, J. Appl. Phys. 99 (2006) 094105.
[11] A. Kumar, I. Rivera, R.S. Katiyar, J.F. Scott, Appl. Phys. Lett. 92 (2008) 132913.
[12] B. Jeyadevan, K. Tohji, K. Natsukasa, J. Appl. Phys. 76 (1994) 6325.
[13] Y.T. Li, Q. Li, M.L. Wen, J. Electron. Spectrosc. Relat. Phenom. 160 (2007) 1.
[14] Deepti Kothari, V. Raghavendra Reddy, et al., J. Phys.: Condens. Matter 22 (2010) 356001.
[15] Dongeun Lee, et al., Appl. Phys. Lett. 86 (2005) 222903.
[16] W.J. Zhong, B. He, J. Univ. Sci. Technol. China 35 (2001) 328.
[17] S.Q. Wei, et al., Phys. Rev. B 63 (2001) 224201.
[18] M. Abbate, F.M.F. de Groot, J.C. Fuggle, A. Fujimori, O. Strebel, F. Lopez, M. Domke, G. Kaindl, et al., Phys. Rev. B 46 (1992) 4511.
[19] Tohru Higuchi, Yi-Sheng Liu, Peng Yao, Per-Anders Glans, Jinghua Guo, et al., Phys. Rev. B 78 (2008) 085106.
[20] J. Wang, A. Scholl, H. Zheng, S.B. Ogale, D. Viehland, D.G. Schlom, N.A. Spaldin, K.M. Rabe, M. Wuttig, L. Mohaddes, J. Neaton, U. Waghmare, T. Zhao, R. Ramesh, Science 307 (2005) 1203b.
[21] Z.C. Quan, W. Liu, H. Hu, S. Xu, B. Sebo, G.J. Fang, M.Y. Li, X.Z. Zhao, J. Appl. Phys. 104 (2008) 084106.
[22] F.Z. Huang, X.M. Lu, W.W. Lin, X.M. Wu, Y. Kan, J.S. Zhu, Appl. Phys. Lett. 89 (2006) 242914.
[23] I. Sosnowska, T.P. Neumaier, E. Steichele, J. Phys. C: Solid State Phys. 15 (1982) 4835.